

Nano Sized Hydroxyapatite-Polylactic Acid-Vancomycin in Alleviation of Chronic Osteomyelitis

Xiao-Feng Lv*, Dong-Ming Zhou, Xiao-Hong Sun*, Ze Zhao

Department of Trauma, First Affiliated Hospital of Baotou Medical College, Inner Mongolia University of Science and Technology, Baotou, Inner Mongolia Autonomous Region, 014010, People's Republic of China

*These authors contributed equally to this work

Correspondence: Dong-Ming Zhou, Department of Trauma, First Affiliated Hospital of Baotou Medical College, Inner Mongolia University of Science and Technology, Baotou, Inner Mongolia Autonomous Region, 014010, People's Republic of China, Tel +86-13171243354, Email zhoudm2982@outlook.com

Background: Vancomycin (VAN) is effective in inhibiting inflammatory reactions in chronic osteomyelitis (CO), while nano-hydroxyapatite (nHA) can effectively address the poor biocompatibility and high brittleness of ordinary HA and better repair bone defects. Therefore, the efficacy of nHA combined with VAN for CO with bone defects deserves further discussion.

Objective: To explore the effect of VAN, which is loaded in the nanodelivery system formed by nHA and polylactic acid (PLA), in CO therapy.

Methods: The stability of nHA-PLA-VAN in PBS solution at different temperatures and its effect on VAN's half-life were determined in the physicochemical property test. Immunofluorescence (IF) determined the stability and permeability of Cy3-coupled nHA-PLA-VAN in bone marrow of B6/J mice. The cultured osteoblasts were further divided into control, polyethyleneimine (PEI), and nHA-PLA groups to observe their differences in cell proliferation, mineralization, and migration capacities. And a CO mouse model was constructed to detect the anti-CO effect of nHA-PLA-VAN.

Results: nHA-PLA-VAN nanocomposites maintained good stability in different acidic solutions, favoring their long-term preservation in vitro. nHA-PLA extended VAN's half-life by 6-times. In the permeation test, nHA-PLA-VAN showed significantly higher permeation efficiency than PEI, enabling it to effectively transport VAN to bone marrow tissue, thus better inhibiting bacterial activity and reducing CD4, CD8, CD19, and CD20 expression in the lesion area of CO mice. In the osteoblast experiment, nHA-PLA more effectively maintained osteoblast viability and promoted proliferation and migration, thus better repairing defective bone tissue. In the CO mouse model, nHA-PLA-VAN better inhibited inflammatory reactions, such as congestion and edema in the focus, and increased the number and thickness of bone trabeculae. Furthermore, max load, elastic load, and rigidity coefficient of the bone defect area were recovered to a great extent.

Conclusion: nHA-PLA-VAN may be a better choice for future treatment of CO.

Keywords: nano-hydroxyapatite, polylactic acid, vancomycin, chronic osteomyelitis

Introduction

Due to the development of the transportation and real estate industry in recent years, the incidence of fall injuries and traffic accidents is increasing year by year. Such patients are often seriously injured, with open fractures of limbs. As the wound is exposed and often complicated with bone defects, infection and delayed healing are prone to occur during treatment, resulting in chronic osteomyelitis (CO).¹ There are dead bones and dead spaces with poor blood supply at the lesion site of patients with CO, which has greatly hindered its treatment.² In terms of CO treatment, complete debridement is required to remove dead bones and dead space. While it is effective in removing dead bones and significantly reducing the amount of bacteria in the focus, it can also cause a large number of bone tissue defects,

which will reduce the stability of bones.^{3,4} In addition, an unsatisfactory bactericidal effect by antibiotics at the lesion site can lead to massive bacterial multiplication, and the emergence of methicillin-resistant *Staphylococcus aureus* (MRSA) further increases the difficulty of CO treatment. At present, gentamicin-polymethyl methacrylate (PMMA) beads have been developed to treat CO with encouraging therapeutic effects achieved. However, its shortcomings are gradually exposed during clinical application. First, PMMA beads need to be removed by a secondary surgery as they cannot be degraded and absorbed *in vivo*, increasing the pain and healing time of patients.⁵ In addition, due to the relatively poor drug loading performance of PMMA, it cannot continuously maintain the concentration of anti-inflammatory drugs in the cavity, which will easily lead to repeated bacterial infections.⁶ Therefore, developing an absorbable biomaterial that can carry antibiotics efficiently for CO treatment is a hot spot in clinical research.

In this study, we selected nano-hydroxyapatite (nHA)-polylactic acid (PLA) composites loaded with vancomycin (VAN) to treat CO. As the main component of bone, HA has become a common bone tissue repair material in clinical orthopedics due to its good osteoconduction and osteoinduction.⁷ However, because of poor toughness, it cannot be used for the repair of weight-bearing bone.⁸ Relevant research has found that the physical properties of HA are closely related to its diameter, and with the decrease of particle size, it can be endowed with elasticity similar to human cortical bone.⁹ Therefore, nHA can address the shortcoming of poor toughness of HA to a certain extent. PLA is a biodegradable material with good *in vivo* compatibility and favorable elasticity,¹⁰ which enables it to be used as a carrier material for bone and cartilage tissue cells regeneration. However, given its poor mechanical strength, it is not suitable to be used alone for bone tissue repair.^{11,12} Otherwise, the accumulation of lactic acid, a metabolite produced by PLA, can easily lead to inflammatory reactions.¹³ In order to overcome the shortcomings of the two materials in repairing bone defects when used alone, we combined them to synthesize a composite material to play a synergistic effect. In this way, while improving the toughness of nHA and making it more consistent with the biomechanical strength of normal bone,¹⁴ it can also buffer the lactic acid produced by PLA metabolism through nHA.¹⁵ In addition, the three-dimensional pore structure of nHA-PLA can provide a good biomimetic skeleton for the proliferation and adhesion of bone cells to contribute to the secretion of extracellular matrix, so as to better promote the growth of new bone.¹⁶

In terms of the selection of antibiotics, the common pathogen of CO is *Staphylococcus aureus*. However, due to the excessive use of antibiotics, its drug resistance has gradually increased, with different degrees of tolerance to penicillin, cephalosporin, and other antibiotics, further increasing the difficulty of CO treatment.¹⁷ Among various antibiotics, VAN is one that is sensitive to MRSA. However, its nephrotoxicity and ototoxicity limit its clinical application. Loading VAN with nHA-PLA can better control its release efficiency, so as to maintain its concentration in the lesion and effectively reduce the systemic toxicity, thus providing a more stable microenvironment for the proliferation of osteocytes. Therefore, this study investigated the therapeutic effect of nHA-PLA-VAN composites in the treatment of CO.

Materials and Methods

nHA-PLA-VAN System Assembling

The whole system contains two elements, which is the nHA-PLA vector outside and loaded VAN inside. The first and the key step is nHA-PLA vector construction. The main protocol was shown as follows: 30-g nHA (N9164, Sigma-Aldrich, MO) was prepared and mixed with 200-mL castor oil (8001794, Sigma-Aldrich) by stirring. Next, 20-g isophorone diisocyanate (2238616, Sigma-Aldrich) was added to the mixture and stirred at 70°C for 3 hours. Then, 2-mL 1,4-butanediol (110634, Sigma-Aldrich) was added to the pre-polymer and stirred for another 1 hour. Finally, the mixture was freeze dried while foaming, which was a key step. Following these steps, the nHA-PLA backbone was made. Subsequently, the prepared VAN (1404939, Sigma-Aldrich) was incubated with the backbone at 40°C for 1.5 hours and dried in a vacuum oven at the same temperature. Finally, the nHA-PLA-VAN system was completed (Figure 1). Polyethyleneimine (PEI) was used to synthesize PEI-VAN as a control, and the synthetic process was conducted as previously reported.¹⁸

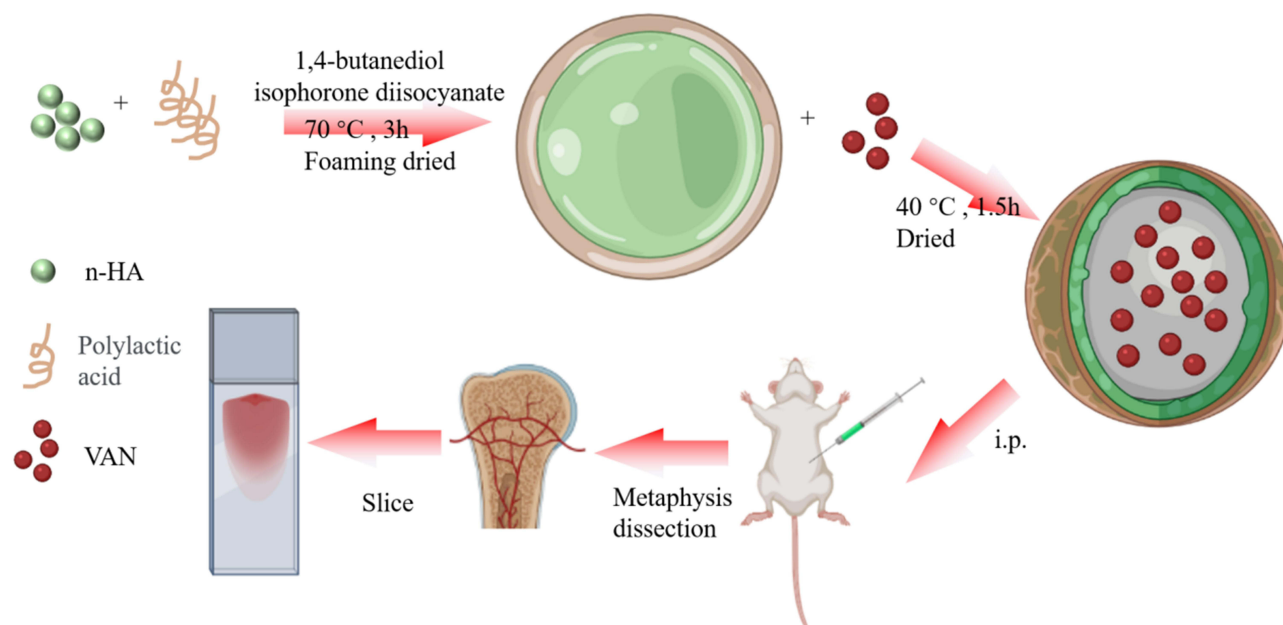


Figure 1 nHA-PLA-VAN system assembling and study strategy.

Physicochemical Property Test of nHA-PLA-VAN

First, synthesized nHA-PLA-VAN was dissolved in a medium containing nitric acid, hydrochloric acid, and Phosphate Buffer Saline to test their diameter at the time points of 0, 24, 48, 72, and 96 hours using scanning electron microscopy. This part mainly tests whether synthesized particles are stable at different mediums. Second, VAN, PEI-VAN, and nHA-PLA-VAN were administered intraperitoneally into C57BL/6 mice of about 25 g in weight. Blood samples were collected per hour from the tail vein of the above-injected mice, and VAN concentration was detected to determine the half-time. Then nHA-PLA-VAN was coupled with Cy3 (777315, Sigma-Aldrich) to test the fluorescence intensity after storing at 0°C, 60°C, and 100°C for 4 hours, and meanwhile, nHA-PLA-VAN dissolved in PBS was stood by for 0, 24, 48, and 72 hours to test how much precipitate will be produced. These two parts were used to test the stability of nHA-PLA-VAN-Cy3 as the Cy3-coupled nHA-PLA-VAN would be used for subsequent experiments.

Permeation Test of nHA-PLA-VAN in Bone Marrow Tissue

Before testing the effect of nHA-PLA-VAN, we need to test its permeation capacity in target tissue. Here we used nHA-PLA-VAN-Cy3 to perform this part. Eight-week-old male B6/J mice purchased from Charles River Company (Beijing, China) were chosen, and PBS-dissolved nHA-PLA-VAN-Cy3 and PEI-VAN-Cy3 were injected in the marrow cavity of femoral diaphysis. After 24 hours, the injected lesion was dissected to evaluate the Cy3 labeled cells. The more and brighter the labeled cells, the better the permeation capacity. The images were processed with a confocal microscope (SP8, Leica, Germany).

nHA-PLA-VAN Test in Cultured Osteoblast Cells

Human osteoblasts (CP-H111, Procell, Wuhan, China) were planted into 24-well plates and cultured in a complete culture medium in a cell incubator (51032124, ThermoFisher, MA) for 24 h under the conditions of 5% CO₂ and 37°C. These cells were then collected and diluted with PBS solution at a concentration of 1×10⁴ cells/mL. The above osteoblasts diluents were divided into PEI-VAN group and nHA-PLA-VAN group. Then PBS-dissolved nHA-PLA-VAN and PEI-VAN were separately added to the above groups, and the evaluation was performed after 7 days. First, we observed the cell density under differential interference contrast (DIC) microscopy. Then, anti-osteoprotegerin (OPG; ab124820, Abcam) and anti-Ki67 (ab15580, Abcam) were added to the culture cells, respectively, to evaluate the number and the

proliferation ability of the cultured osteoblasts. Each kind of cell number was calculated by counting the average number in three high-power fields (HPFs, 40×). For the migration test, a sterilized pipette tip was used to make a scratch on the surface of cells in each group, and the cells at the scratch were washed with PBS. After 24 hours of culture, the migration of osteoblasts at the scratch was observed under the microscope, and cell number under each HPF was also counted. A total of three HPFs were counted in each group to take the average value.

CO Mouse Model Construction

Eight-week-old male B6/J mice were used for CO model construction. To ensure success modeling, we selected 12 mice with a weight of 24–25 g as candidates for model construction. First, these mice were anesthetized with isoflurane, and an incision was made on the skin of the right knee. Then we exposed the end of femur and used a drill to perforate the end of femur. A 1- μ L medium containing 1×10^8 *Staphylococcus aureus* was then injected into the marrow cavity produced by the drill. Then bone wax was used to fill the lesion and all the post-surgical mice were warmed on a heating pad until they could move again. After 4 weeks, the CO mice were established. Nine out of the 12 mice were chosen and divided into three groups randomly. Then saline, PEI-VAN, and nHA-PLA-VAN were injected in the lesion of CO mice every 3 days, respectively, lasting for 2 weeks. The experiment, approved by the Experimental Animal Ethics Committee of the First Affiliated Hospital of Baotou Medical College, Inner Mongolia University of Science and Technology, was conducted in accordance with the Chinese guidelines specified in the Guide for the Care and Use of Laboratory Animals.

Lymphocytes Evaluation in Lesions of CO Mice

As lymphocytes are typical proliferated inflammatory cells in CO, we first evaluated change in lymphocyte counts in these mice with different treatments. Anti-CD4 (ab183685, Abcam) and anti-CD8 (ab217344, Abcam) were used to label T lymphocytes while anti-CD19V (ab245235, Abcam) and anti-CD20 (ab78237, Abcam) were used to label B lymphocytes. The count of each lymphocyte subset was also obtained by counting the average number in three HPFs (40×).

Treatment Effect Evaluation of nHA-PLA-VAN

After saline, PEI-VAN, or nHA-PLA-VAN injection that was performed every 3 days for 12 weeks, the treated mice were sacrificed and the injected lesions were dissected. First, their macroscopic images, including the hemorrhage, swelling, and inflammation, were observed. The lesions were then made into slices for HE staining, and their trabecular number and trabecular thickness were evaluated under microscopy. Each index was determined by counting the average number in three HPFs (40×).

Bone Mechanical Force Measurement

The right femur of mice in each group was collected and bone surface muscles were removed for biomechanical experiments. Then, the three-point bending load of femoral specimens was detected with an electronic universal testing machine (AG-IC50kN, Shimadzu instrument (Suzhou) Co., Ltd.). Before testing, a vernier caliper was used to measure the long and short diameters of femoral metaphysis, and the short diameter should be kept consistent with the direction of loading force. The relevant parameters were set as follows: loading rate: 9 mm/min, test span: 9 mm, and measurement range: 0–1,000 N. Eventually, the Max load, Elasticity load, and Rigidity coefficient were detected to judge the mechanical force of the femur of mice in each group relative to that of normal mice.

Results and Discussion

Physicochemical Property Test of nHA-PLA-VAN

Before applying nHA-PLA-VAN as a method to treat CO, we need to test its physicochemical property to guarantee its feasibility. First, we measured the diameter of the composites treated with different mediums for as long as 96 hours, and found the particles remained at 100 nm in size with almost no changes (Figure 2A), suggesting that the synthesized particles have very stable size in different mediums. Second, both the two nanocarriers could effectively extend the half-

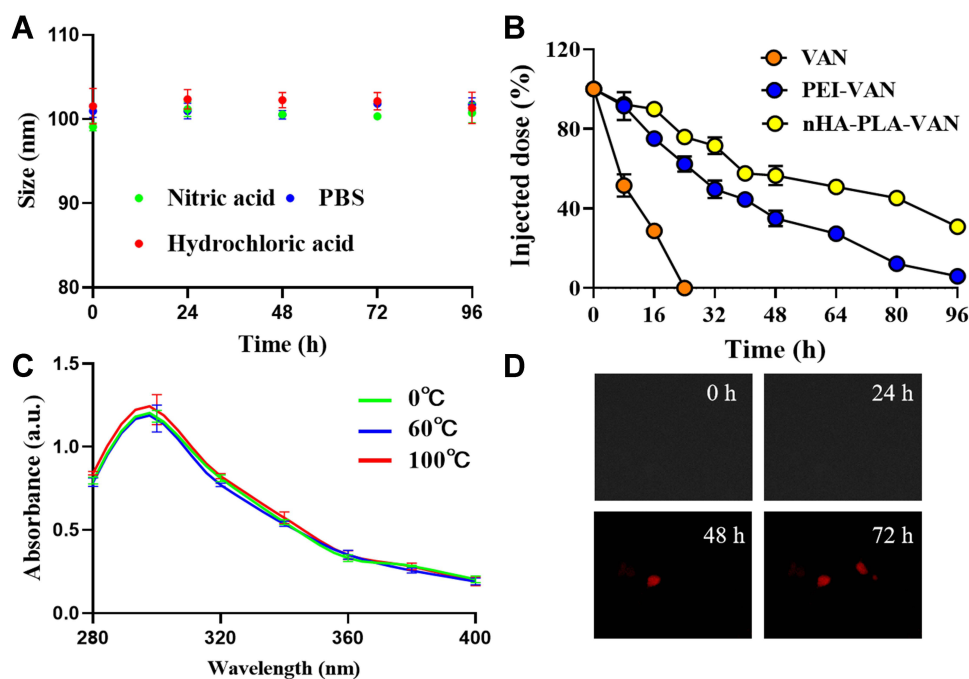


Figure 2 Physicochemical property test of nHA-PLA-VAN. (A) Size of nHA-PLA-VAN at different mediums observed under a scanning electron microscope. (B) Half-life test after nHA-PLA-VAN, PEI-VAN and pure VAN injection. (C) Fluorescence absorbance of nHA-PLA-VAN-Cy3 at different temperatures. (D) Precipitates of nHA-PLA-VAN-Cy3 after standing in PBS for certain hours.

life of VAN, especially in the nHA-PLA-VAN group (Figure 2B). Then the particles were coupled with Cy3 to test their fluorescence binding capacity by measuring the fluorescence absorbance and stability in medium by precipitate images. It showed that the coupled nHA-PLA-VAN-FITC has the same strongest emission wavelength (approximately 650 nm) as Cy3, even when stored at different temperatures (Figure 2C). When dissolved in PBS, only several precipitates could be detected after 48 hours (Figure 2D). These two results showed that nHA-PLA-VAN can bind with fluorescein stably without changing the characteristics of the bound fluorescein and rarely accumulates to precipitate. Considering its favorable stability, nHA-PLA-VAN can be applied for further tests.

Permeation Capacity of nHA-PLA-VAN-Cy3 in Bone Marrow Tissue

Second, we tested the permeation capacity of nHA-PLA-VAN to identify its target efficiency. nHA-PLA-VAN-Cy3 was injected into the marrow cavity of CO mice and, 24 hours later, the injected lesions were dissected to evaluate the Cy3 labeled cells. The PEI-VAN-Cy3 was used as control. nHA-PLA-VAN-Cy3 was found to successfully and more effectively label cells in the marrow cavity, indicating nHA-PLA delivered more VAN into cells (Figure 3). Hence, nHA-PLA-VAN does have the capacity to deliver more VAN to target cells.

nHA-PLA-VAN Inhibits Lymphocytes in Lesions of CO Mice

As mentioned before, lymphocytes are typical proliferated inflammatory cells in CO, so we evaluated changes in the counts of lymphocyte subsets in mice treated with PEI-VAN or nHA-PLA-VAN to evaluate their effects on inflammation. The results showed that nHA-PLA-VAN more significantly decreased labeled CD4 and CD8 T lymphocytes in lesions of CO mice than PEI-VAN (Figure 4A–D). The same conclusion was obtained in terms of the counts of labeled B lymphocytes CD19 and CD20 (Figure 4E–H). The quantitative data was presented in Figure 4I. Therefore, we believe that nHA-PLA-VAN can successfully inhibit inflammation in CO mice.

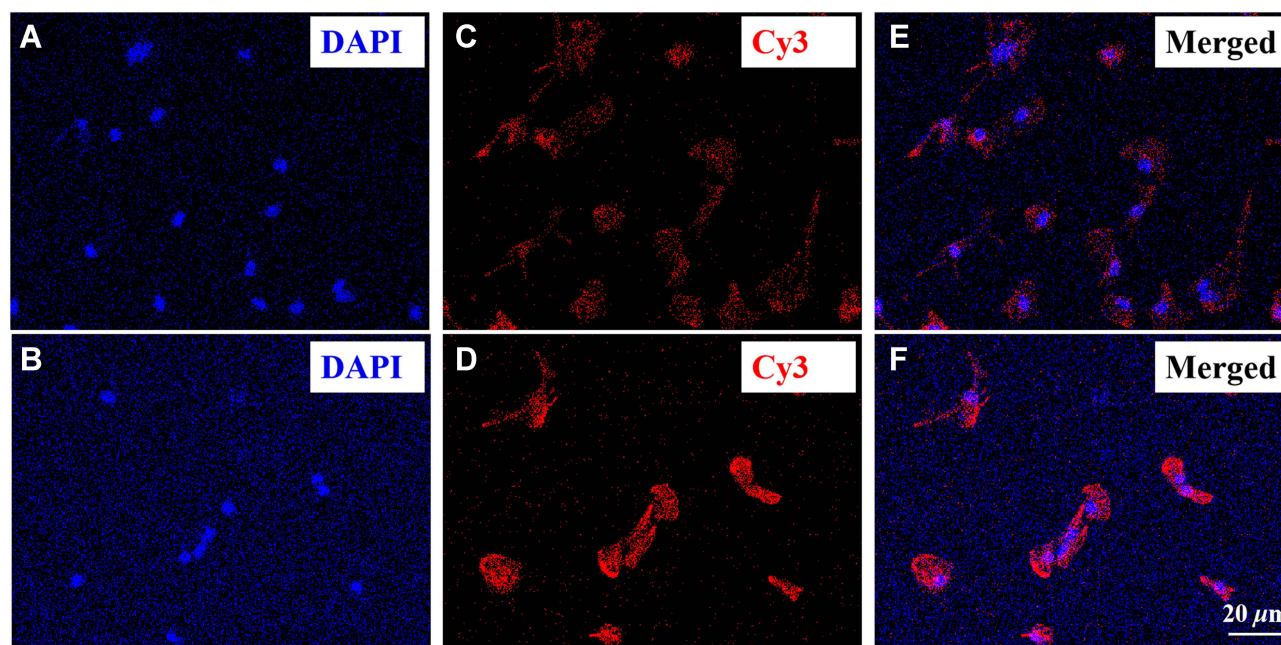


Figure 3 Permeation ability of nHA-PLA-VAN-Cy3 in bone marrow tissue. (A) DAPI staining of bone marrow tissue treated with PEI-VAN, $\times 20$. (B) DAPI staining of bone marrow tissue treated with nHA-PLA-VAN, $\times 20$. (C) Cy3 expression in bone marrow tissue treated with PEI-VAN, $\times 20$. (D) Cy3 expression in bone marrow tissue treated with nHA-PLA-VAN, $\times 20$. (E) Merged image of bone marrow tissue treated with PEI-VAN, $\times 20$. (F) Merged image of bone marrow tissue treated with nHA-PLA-VAN, $\times 20$.

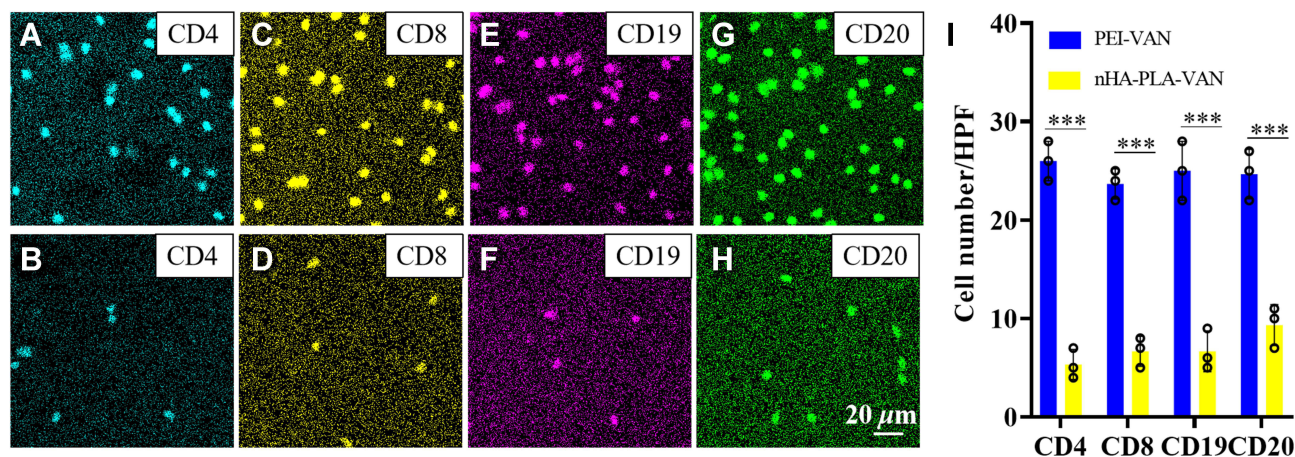


Figure 4 Inhibition ability of nHA-PLA-VAN on Lymphocytes in CO lesions of mice. (A) Anti-CD4-labeled T lymphocytes treated with PEI-VAN, $\times 20$. (B) Anti-CD4-labeled T lymphocytes treated with nHA-PLA-VAN, $\times 20$. (C) Anti-CD8-labeled T lymphocytes treated with PEI-VAN, $\times 20$. (D) Anti-CD8-labeled T lymphocytes treated with nHA-PLA-VAN, $\times 20$. (E) Anti-CD19-labeled B lymphocytes treated with PEI-VAN, $\times 20$. (F) Anti-CD19-labeled B lymphocytes treated with nHA-PLA-VAN, $\times 20$. (G) Anti-CD20-labeled B lymphocytes treated with PEI-VAN, $\times 20$. (H) Anti-CD20-labeled B lymphocytes treated with nHA-PLA-VAN, $\times 20$. (I) Cell number of labeled T and B lymphocytes treated with PEI-VAN or nHA-PLA-VAN. *** $P < 0.001$.

nHA-PLA-VAN Can Keep Cultured Osteoblast Cells Alive and Proliferate

As maintenance of osteoblast growth should be part of CO therapy, we test the role of nHA-PLA-VAN in cultured osteoblasts. It was found that nHA-PLA-VAN was better than PEI in increasing the number of cultured osteoblasts under DIC (Figure 5A and B). The osteoblasts treated with nHA-PLA-VAN could better express OPG, a marker of osteoblasts (Figure 5C and D), and tend to proliferate much better than cells treated with PEI-VAN (Figure 5E and F). The quantitative cell number under DIC and the expression of OPG and Ki67 are presented in Figure 5G. The above data show that nHA-PLA-VAN can better keep cultured osteoblast cells alive and maintain their proliferation.

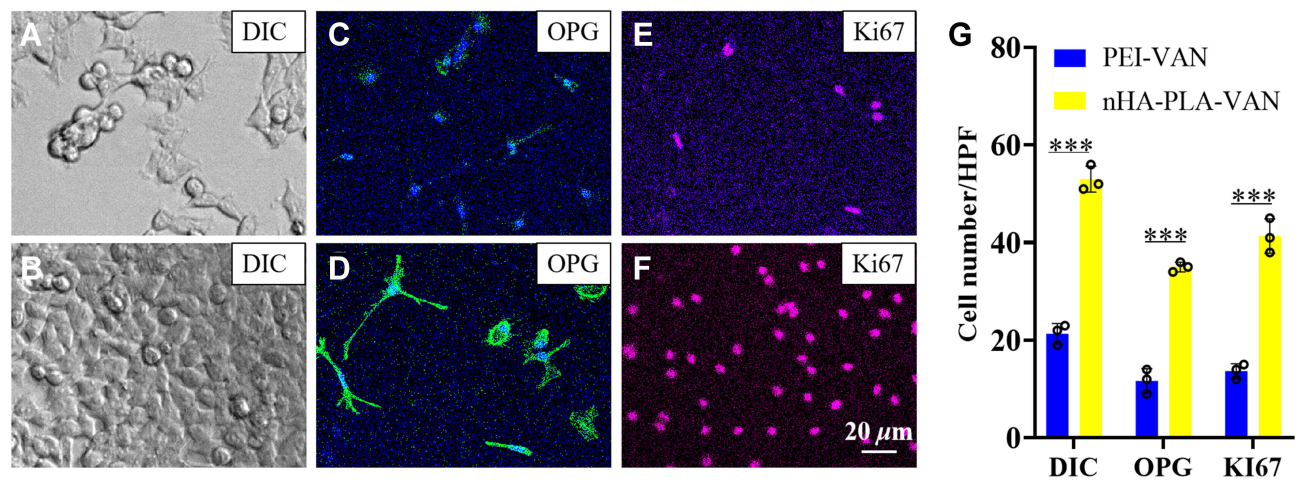


Figure 5 Viability of osteoblasts. (A) Viability of osteoblasts treated with PEI-VAN under DIC, $\times 20$. (B) Viability of osteoblasts treated with nHA-PLA-VAN under DIC, $\times 20$. (C) Anti-OPG expression pattern in osteoblasts treated with PEI-VAN, $\times 20$. (D) Anti-OPG expression pattern in osteoblasts treated with nHA-PLA-VAN, $\times 20$. (E) Anti-Ki67 expression pattern in osteoblasts treated with PEI-VAN, $\times 20$. (F) Anti-Ki67 expression pattern in osteoblasts treated with nHA-PLA-VAN, $\times 20$. (G) Cell number per high power field (HPF, $40\times$) under DIC, as well as anti-OPG and anti-Ki67 expression of osteoblasts treated with PEI-VAN or nHA-PLA-VAN. *** $P < 0.001$.

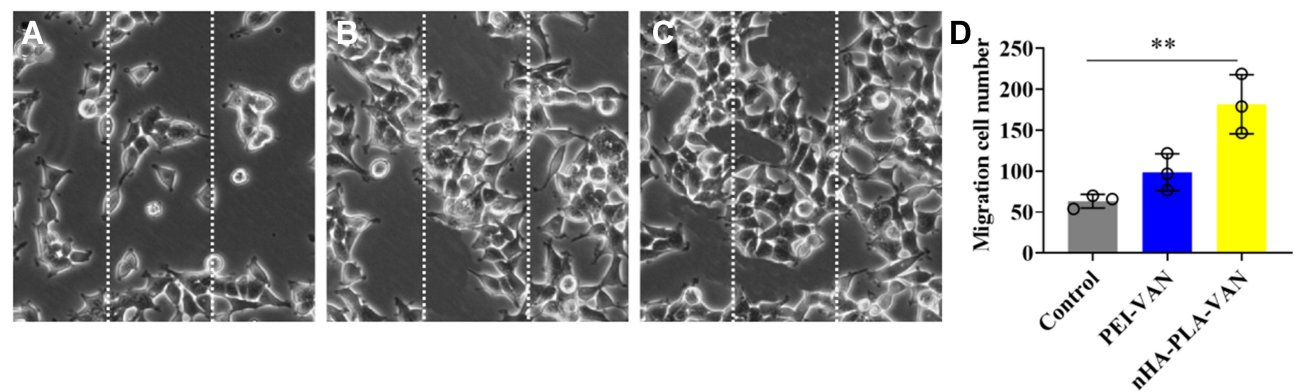


Figure 6 Scratch test of osteoblasts in different groups. (A) Migration of osteoblasts treated with saline; (B) Migration of osteoblasts treated with PEI-VAN; (C) Migration of osteoblasts treated with nHA-PLA-VAN. (D) Quantitative evaluation of osteoblast migration number in control, PEI-VAN, and nHA-PLA-VAN groups. ** $P < 0.01$.

nHA-PLA-VAN Promotes Osteoblast Migration

The migration ability of osteoblasts, an important index affecting the repair of bone injury, can effectively reflect the repair effect of CO with bone defects. As shown in Figure 6A–C, osteoblasts treated with PEI-VAN or nHA-PLA-VAN migrated more to the scratch area, especially in the nHA-PLA-VAN group. In the quantitative analysis, the number of osteoblasts treated with nHA-PLA-VAN in each HPF was also the highest (Figure 6D). Therefore, nHA-PLA-VAN can better guide osteoblast migration, so as to effectively repair CO combined with bone defects.

nHA-PLA-VAN Alleviates CO

At last, we evaluate the effect of nHA-PLA-VAN in the treatment of CO mice. As expected, nHA-PLA-VAN better alleviated the lesions in CO mice after 12 weeks with clean appearance and less swelling and hemorrhage, while saline injection left a typical CO appearance, including bleeding, swelling, and dirty looking, and PEI-VAN only partly improved the lesions (Figure 7A). Under microscopic images of HE staining, we calculated the trabecular number and measured the trabecular thickness. It was found that CO mice treated with nHA-PLA-VAN had the highest trabecular number and the thickest trabecular than those treated with PEI-VAN or saline (Figure 7B and C). Therefore, we believe that nHA-PLA-VAN can better alleviate OC in mouse models.

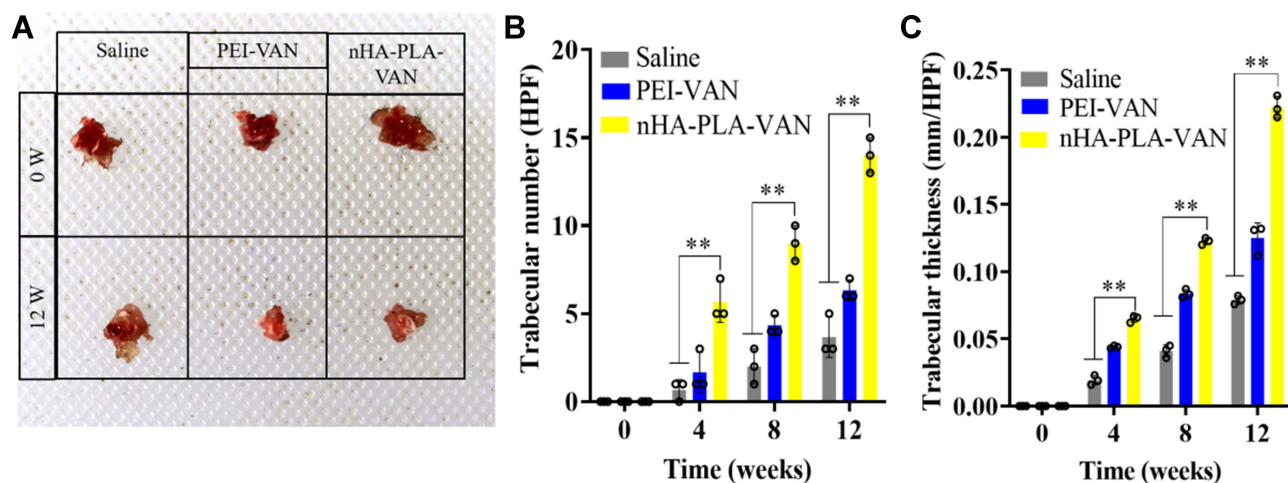


Figure 7 Therapeutic effect of nHA-PLA-VAN in the treatment of CO. **(A)** Macroscopic appearance of lesions in CO mice treated with saline, PEI-VAN, or nHA-PLA-VAN. **(B)** Trabecular number of lesions in CO mice treated with saline, PEI-VAN or nHA-PLA-VAN. **(C)** Trabecular thickness of lesions in CO mice treated with saline, PEI-VAN, or nHA-PLA-VAN. ** $P < 0.01$.

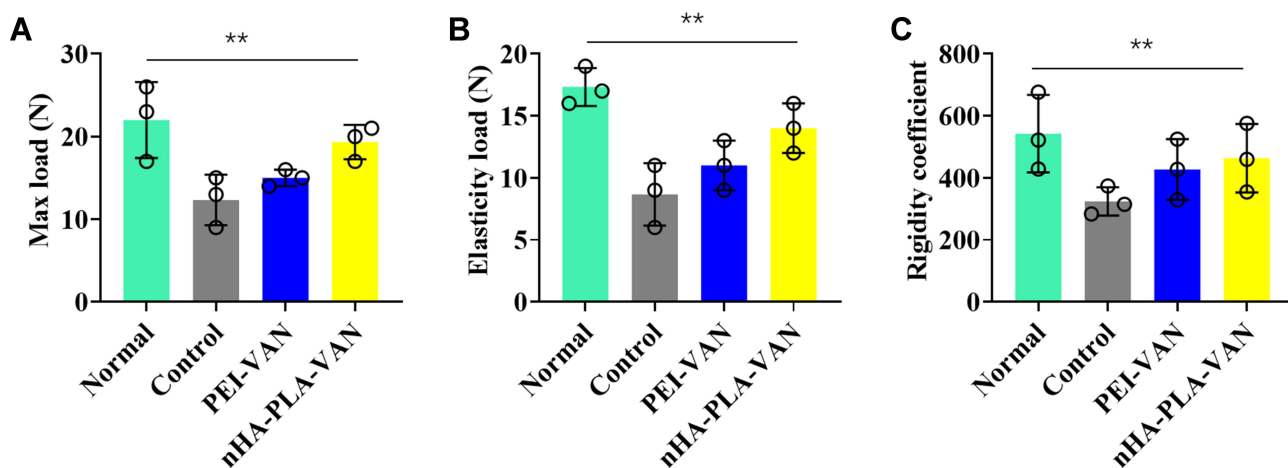


Figure 8 Biomechanical property detection of the femur of mice in different groups. **(A)** Max load detection in normal mice, as well as CO mice treated with saline, PEI-VAN, or nHA-PLA-VAN. **(B)** Elasticity load detection in normal mice, as well as CO mice treated with saline, PEI-VAN, or nHA-PLA-VAN. **(C)** Rigidity coefficient detection in normal mice, as well as CO mice treated with saline, PEI-VAN, or nHA-PLA-VAN. ** $P < 0.01$.

nHA-PLA-VAN Better Restores Bone Biomechanical Properties of CO Mice

The bone biomechanical test can effectively reflect the recovery of bone tissue strength and hardness evaluated from Max load, Elasticity load, and Rigidity coefficient in CO mice after treatment. As shown in Figure 8, after treatment, the above indexes were better improved in PEI-VAN and nHA-PLA-VAN groups, with those in the nHA-PLA-VAN group closer to those in the normal group. Therefore, nHA-PLA-VAN can better treat CO and restore the compression and deformation resistance of bone tissue.

Discussion

Characterized by easy recurrence, long disease course, and difficult therapy,¹⁹ CO has long been a difficulty in clinical orthopedics. Worse still, the continuous emergence of pathogen resistant strains in recent years further complicates its treatment.²⁰ At present, CO treatment is mainly based on debridement, elimination of dead bone and dead space, and antibiotic therapy.²¹ Therefore, after thorough debridement, it is a hotspot in clinical research to find a composite material with good biomechanical strength and biocompatibility, as well as degradable absorption for repairing bone defects.²² In

addition, the antibiotic sustained-release system of the composite material can effectively maintain a high concentration of antibiotics in the focus, and reduce systemic toxic and side-effects, thus significantly reducing the hospitalization time and treatment costs of patients.²³ With the progress of bioengineering technology, more and more new materials have been synthesized and found, which provides more possibilities for the selection of artificial bone materials for CO patients.

nHA-PLA-VAN composites, which have the osteoinduction of nHA, were synthesized in this study to treat CO. When it is placed in the defect after debridement in CO patients, bone cells and blood vessels will gradually grow from the bridged parts at both ends of the material to form the original structure of bone tissue.²⁴ At the same time, the osteoinduction property of nHA can make osteoblasts adhere and proliferate around and inside the composite, which greatly accelerates the healing of bone tissue.²⁵ The addition of PLA further improves the flexibility of nHA,²⁶ which makes the composite more consistent with the mechanical properties of human bone, allowing it to be a better filling material for load-bearing bone. On the other hand, when VAN is loaded on nHA-PLA, its half-life can be effectively extended. According to statistics, even after *in vivo* application of nHA-VAN for 4 weeks, the concentration of VAN in the wound is still higher than its minimum inhibitory concentration.²⁷ The continuous release of VAN creates favorable conditions for the proliferation and repair of osteoblasts. Therefore, the combination of the two can maintain their advantages while effectively overcoming the shortcomings when they are used as bone graft materials alone. Hence, it has become a new drug carrier that perfectly combines osteoconduction, osteoinduction, mechanical strength, and sustained release.^{28,29} In the physical properties study of nHA-PLA-VAN, it was found that it can maintain good stability in different acidic solutions *in vitro*, which is conducive to its long-term preservation. In addition, Cy3 fluorescent dye can be closely bound to nHA-PLA-VAN without changing the characteristics of fluorescein, indicating its feasibility for subsequent experimental research.

In the treatment of CO, it is of great significance to continuously inhibit bacterial infection in the focus and remove hidden bacteria in normal bone tissue after debridement. This not only requires VAN to form a high local concentration within the lesion, but also needs it to further penetrate into the bone marrow tissue to eliminate hidden bacteria. The study found that, compared with the PEI-VAN drug delivery system, nHA-PLA-VAN could more effectively penetrate into bone marrow to continuously release VAN inside the focus, thus completely eliminating the bacteria. In the subsequent detection of lymph nodes number in the focus, it was found that CD4⁺, CD8⁺, CD19⁺, and CD20⁺ counts decreased more significantly after nHA-PLA-VAN treatment. As an important cellular component of immune response *in vivo*, lymphocytes play an important role in fighting against bacterial infection. CD4⁺ T lymphocytes can inhibit bacterial proliferation by secreting cytokines, and CD8⁺ T lymphocytes mainly kill bacteria through cytotoxicity. Furthermore, CD19⁺ and CD20⁺ B lymphocytes can prevent pathogen adsorption and infection through humoral immunity and cytotoxicity. Therefore, the decrease of the above lymphocyte levels further suggests that nHA-PLA-VAN can better eliminate pathogens in the lesions, and gradually stabilizes the immune response *in vivo*.

Promoting the formation of new bone and restoring the load-bearing and stability of bone tissue at sites with bone defects are also keys of CO treatment. In addition to the good biomechanical properties, nHA-PLA-VAN with a three-dimensional hole like structure similar to human cancellous bone, is found to better promote the adhesion of osteoblasts, and provide a wide surface area and internal space for the secretion of extracellular matrix. Therefore, in the proliferation experiment of osteoblasts *in vitro*, we found that osteoblasts cultured with nHA-PLA were more closely distributed with higher proliferation and fewer apoptosis cells, suggesting that nHA-PLA is a good carrier for osteoblast adhesion and growth. And, thanks to the good bone conduction of nHA-PLA, it better guides osteoblasts to migrate to the nHA-PLA scaffold, thus facilitating the repair of bone defects. In order to further investigate the therapeutic effect of nHA-PLA, we carried out experiments using the CO mouse model. In the repair of bone morphology and structure, the study found that nHA-PLA-VAN better alleviated and repaired the damage in the focus, effectively curbed inflammatory reactions such as congestion and edema, and significantly increased the number and thickness of bone trabeculae, contributing to effective repair of the bone defect in the focus. Furthermore, in terms of restoring the biomechanical properties of bone tissue, nHA-PLA-VAN was found to better improve the Max load, Elastic load, and Rigidity coefficient of bone defect area, suggesting that it can effectively restore the strength and hardness of bone tissue.

Conclusion

In this study, we used nHA-PLA as a nano drug loading device of VAN to test its therapeutic effect in CO. It was found that nHA-PLA-VAN had good stability in vitro, which was beneficial to its preservation. In vivo, nHA-PLA shows good biocompatibility and degradability. In addition, it can effectively release VAN in the focus and transport it to bone marrow tissue, so as to better sterilize and inhibit the occurrence of inflammatory reaction. At the same time, the favorable osteoconduction and osteoinduction of nHA-PLA-VAN help to promote the adhesion, proliferation, and migration of osteoblasts, so as to better repair bone defects. In the CO mice model, we found that nHA-PLA-VAN could better reduce inflammatory responses such as congestion and edema in the focus, and promote the construction of cancellous bone in the medullary cavity, contributing to better restored biomechanical properties of bone. Therefore, nHA-PLA-VAN may be a better choice for the treatment of CO in the future.

Data Sharing Statement

The labeled dataset used to support the findings of this study are available from the corresponding author upon request.

Funding

Project Description of health and Family Planning Scientific Research Plan of Autonomous Region in 2017, Project Number: 201703162 Project Name: Development and clinical application of a splintered leg surgical stent.

Disclosure

The authors declare no competing interests in this work.

References

1. Spellberg B, Lipsky BA. Systemic antibiotic therapy for chronic osteomyelitis in adults. *Clin Infect Dis*. 2012;54(3):393–407. doi:10.1093/cid/cir842
2. Dym H, Zeidan J. Microbiology of acute and chronic osteomyelitis and antibiotic treatment. *Dent Clin North Am*. 2017;61(2):271–282. doi:10.1016/j.cden.2016.12.001
3. Zhao Y, Ferguson PJ. Chronic nonbacterial osteomyelitis and chronic recurrent multifocal osteomyelitis in children. *Pediatr Clin North Am*. 2018;65(4):783–800. doi:10.1016/j.pcl.2018.04.003
4. Taddio A, Ferrara G, Insalaco A, et al. Dealing with chronic non-bacterial osteomyelitis: a practical approach. *Pediatr Rheumatol Online J*. 2017;15(1):87–94. doi:10.1186/s12969-017-0216-7
5. Luo S, Jiang T, Yang Y, Yang X, Zhao J. Combination therapy with vancomycin-loaded calcium sulfate and vancomycin-loaded PMMA in the treatment of chronic osteomyelitis. *BMC Musculoskelet Disord*. 2016;17(1):502–513. doi:10.1186/s12891-016-1352-9
6. Alonge TO, Ogunlade SO, Omololu AB, Fashina AN, Oluwatosin A. Management of chronic osteomyelitis in a developing country using ceftriaxone-PMMA beads: an initial study. *Int J Clin Pract*. 2002;56(3):181–183.
7. Wong SC, Baji A. Fracture strength and adhesive strength of hydroxyapatite-filled polycaprolactone. *J Mater Sci Mater Med*. 2008;19(2):929–936. doi:10.1007/s10856-007-3016-7
8. Kohyama K, Morishima Y, Arisawa K, Arisawa Y, Kato H. Immediate and long-term results of unsintered hydroxyapatite and poly L-lactide composite sheets for orbital wall fracture reconstruction. *J Plast Reconstr Aesthet Surg*. 2018;71(7):1069–1075. doi:10.1016/j.bjps.2018.03.006
9. Wei X, Egawa S, Matsumoto R, et al. Augmentation of fracture healing by hydroxyapatite/collagen paste and bone morphogenetic protein-2 evaluated using a rat femur osteotomy model. *J Orthop Res*. 2018;36(1):129–137. doi:10.1002/jor.23646
10. Schliephake H, Weich HA, Dullin C, Gruber R, Frahse S. Mandibular bone repair by implantation of rhBMP-2 in a slow release carrier of poly(lactic acid)—an experimental study in rats. *Biomaterials*. 2008;29(1):103–110. doi:10.1016/j.biomaterials.2007.09.019
11. Velioglu ZB, Pulat D, Demirbakan B, Ozcan B, Bayrak E, Eriskan C. 3D-printed poly(lactic acid) scaffolds for trabecular bone repair and regeneration: scaffold and native bone characterization. *Connect Tissue Res*. 2019;60(3):274–282. doi:10.1080/03008207.2018.1499732
12. Tajbakhsh S, Hajiali F. A comprehensive study on the fabrication and properties of biocomposites of poly(lactic acid)/ceramics for bone tissue engineering. *Mater Sci Eng C Mater Biol Appl*. 2017;70(Pt 1):897–912. doi:10.1016/j.msec.2016.09.008
13. Polimeni G, Koo KT, Pringle GA, Agelan A, Safadi FF, Wikesjö UM. Histopathological observations of a poly(lactic acid)-based device intended for guided bone/tissue regeneration. *Clin Implant Dent Relat Res*. 2008;10(2):99–105. doi:10.1111/j.1708-8208.2007.00067.x
14. Ma B, Han J, Zhang S, et al. Hydroxyapatite nanobelt/poly(lactic acid) Janus membrane with osteoinduction/barrier dual functions for precise bone defect repair. *Acta Biomater*. 2018;71:108–117. doi:10.1016/j.actbio.2018.02.033
15. Cai X, Tong H, Shen X, Chen W, Yan J, Hu J. Preparation and characterization of homogeneous chitosan-poly(lactic acid)/hydroxyapatite nanocomposite for bone tissue engineering and evaluation of its mechanical properties. *Acta Biomater*. 2009;5(7):2693–2703. doi:10.1016/j.actbio.2009.03.005
16. Liuyun J, Lixin J, Chengdong X, Lijuan X, Ye L. Effect of l-lysine-assisted surface grafting for nano-hydroxyapatite on mechanical properties and in vitro bioactivity of poly(lactic acid-co-glycolic acid). *J Biomater Appl*. 2016;30(6):750–758. doi:10.1177/0885328215584491

17. Poepl W, Lingscheid T, Bernitzky D, et al. Efficacy of fosfomycin compared to vancomycin in treatment of implant-associated chronic methicillin-resistant staphylococcus aureus osteomyelitis in rats. *Antimicrob Agents Chemother.* 2014;58(9):5111–5116. doi:10.1128/AAC.02720-13
18. Calixto G, Victorelli FD, Dovigo LN, Chorilli M. Polyethyleneimine and chitosan polymer-based mucoadhesive liquid crystalline systems intended for buccal drug delivery. *AAPS PharmSciTech.* 2018;19(2):820–836. doi:10.1208/s12249-017-0890-2
19. Beck-Broichsitter BE, Smeets R, Heiland M. Current concepts in pathogenesis of acute and chronic osteomyelitis. *Curr Opin Infect Dis.* 2015;28(3):240–245. doi:10.1097/QCO.0000000000000155
20. Kinik H, Karaduman M. Ciorny-Mader Type III chronic osteomyelitis: the results of patients treated with debridement, irrigation, vancomycin beads and systemic antibiotics. *Int Orthop.* 2008;32(4):551–558. doi:10.1007/s00264-007-0342-9
21. Conterno LO, Turchi MD. Antibiotics for treating chronic osteomyelitis in adults. *Cochrane Database Syst Rev.* 2013. doi:10.1002/14651858.CD004439.pub3
22. Cox AJ, Zhao Y, Ferguson PJ. Chronic Recurrent Multifocal Osteomyelitis and Related Diseases-Update on Pathogenesis. *Curr Rheumatol Rep.* 2017;19(4):18–23. doi:10.1007/s11926-017-0645-9
23. Joosten U, Joist A, Gosheger G, Liljenqvist U, Brandt B, von Eiff C. Effectiveness of hydroxyapatite-vancomycin bone cement in the treatment of Staphylococcus aureus induced chronic osteomyelitis. *Biomaterials.* 2005;26(25):5251–5258. doi:10.1016/j.biomaterials.2005.01.001
24. Capello WN, D', Antonio JA, Naughton M. Periprosthetic fractures around a cementless hydroxyapatite-coated implant: a new fracture pattern is described. *Clin Orthop Relat Res.* 2014;472(2):604–610. doi:10.1007/s11999-013-3137-x
25. Miller L, Guerra AB, Bidros RS, Trahan C, Baratta R, Metzinger SE. A comparison of resistance to fracture among four commercially available forms of hydroxyapatite cement. *Ann Plast Surg.* 2005;55(1):87–92. doi:10.1097/01.sap.0000162510.05196.c6
26. Kiziltas A, Nazari B, Erbas Kiziltas E, Gardner DJ, Han Y, Rushing TS. Method to reinforce polylactic acid with cellulose nanofibers via a polyhydroxybutyrate carrier system. *Carbohydr Polym.* 2016;140:393–399. doi:10.1016/j.carbpol.2015.12.059
27. Jiang JL, Li YF, Fang TL, et al. Vancomycin-loaded nano-hydroxyapatite pellets to treat MRSA-induced chronic osteomyelitis with bone defect in rabbits. *Inflamm Res.* 2012;61(3):207–215. doi:10.1007/s00011-011-0402-x
28. Lv Q, Nair L, Laurencin CT. Fabrication, characterization, and in vitro evaluation of poly(lactic acid glycolic acid)/nano-hydroxyapatite composite microsphere-based scaffolds for bone tissue engineering in rotating bioreactors. *J Biomed Mater Res A.* 2009;91(3):679–691. doi:10.1002/jbm.a.32302
29. Shebi A, Lisa S. Pectin mediated synthesis of nano hydroxyapatite-decorated poly(lactic acid) honeycomb membranes for tissue engineering. *Carbohydr Polym.* 2018;201:39–47. doi:10.1016/j.carbpol.2018.08.012

Drug Design, Development and Therapy

Dovepress

Publish your work in this journal

Drug Design, Development and Therapy is an international, peer-reviewed open-access journal that spans the spectrum of drug design and development through to clinical applications. Clinical outcomes, patient safety, and programs for the development and effective, safe, and sustained use of medicines are a feature of the journal, which has also been accepted for indexing on PubMed Central. The manuscript management system is completely online and includes a very quick and fair peer-review system, which is all easy to use. Visit <http://www.dovepress.com/testimonials.php> to read real quotes from published authors.

Submit your manuscript here: <https://www.dovepress.com/drug-design-development-and-therapy-journal>